

IMECE2006-15436

DESIGN OF AUTOMOTIVE TORSION BEAM SUSPENSION USING LUMPED-COMPLIANCE LINKAGE MODEL

Naesung Lyu
Dept. of Mechanical Engineering
Univ. of Michigan
Ann Arbor, MI
nlyu@umich.edu

Jungkap Park
Dept. of Mechanical Engineering
Univ. of Michigan
Ann Arbor, MI
jungkap@umich.edu

Hiroyuki Urabe
Automobile R&D Center
Honda R&D Co., Ltd.
Tochigi, Japan
hiroyuki_urabe@n.t.rd.honda.co.jp

Hiroyuki Tokunaga
Automobile R&D Center
Honda R&D Co., Ltd.
Tochigi, Japan
hiroyuki_tokunaga@n.t.rd.honda.co.jp

Kazuhiro Saitou
Dept. of Mechanical Engineering
Univ. of Michigan
Ann Arbor, MI
kazu@umich.edu

ABSTRACT

This paper presents a new method for efficiently and accurately modeling the elasto-kinematic behaviors of torsion beam suspension systems and of other similar classes of mechanical systems, and a design method utilizing the models. The torsion beam is represented as a linkage of lumped mass joined by nonlinear springs, bending and torsion, whose stiffness are identified via off-line computational experiments using nonlinear finite element simulations. A number of such computer experiments are conducted off-line for representative dimensions of torsion beams, and the results are stored in surrogate response models. During design iterations, these surrogate response models are utilized to automatically construct a lumped-compliance linkage model of a torsion beam and integrate it into a multi-body suspension system model that can be simulated using commercial software. Comparison with a nonlinear finite element analysis demonstrates much improved accuracy of the proposed model over commercial flexible multi-body simulation software, with comparable computational speed. Finally, an example is presented on the multi-objective optimization of the cross section of the torsion beam using the developed surrogate response models.

1. INTRODUCTION

Automotive suspension systems provide compliant connections between vehicle body structures and wheel axles. They play a key role in determining the vibration, handling, and maneuverability of a vehicle. Since driving characters of vehicles (*eg.*, sporty and luxury) are largely affected by its vibration, handling, and maneuverability, the design of suspension systems requires fine-tuning to meet the desired performance targets. For this, flexible multi-body simulation

software (*eg.*, MSC.ADAMS [1]) is typically employed for accurately predicting the elasto-kinematic behavior of suspension systems during the vehicle operations.

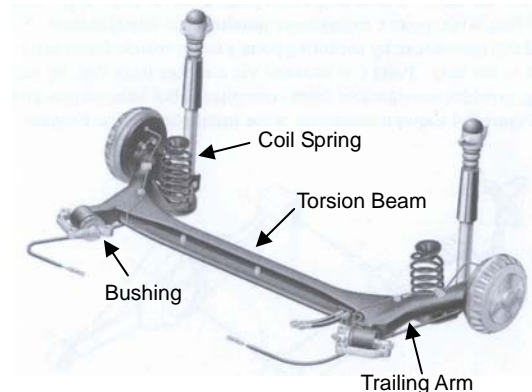


Figure 1. Typical torsion beam rear suspension [2].

Torsion beam suspensions (Figure 1) are widely used as rear wheel suspension systems for front wheel driven passenger vehicles with small to medium sizes, since their simplicity and small number of components can offer maximum space utilization with low cost. Despite its simplicity, the accurate simulation of torsion bar suspension system requires time consuming nonlinear finite element analyses, since the torsion beam undergoes significant nonlinear torsion displacement, which cannot be accurately predicted using the conventional flexible multi-body simulation. This, coupled with the fact that finite element analyses require detailed component geometry, prohibits the effective exploration of design alternatives during the early stage of the suspension design. Since suspension systems are typically designed concurrently with the other

interdependent vehicle subsystems, quick turnarounds for “what-if” scenarios without the need of constructing detailed finite element models is essential for the reduction of the development time [3].

Accordingly, this paper presents a new method for efficiently and accurately modeling the elasto-kinematic behaviors of torsion beam suspension systems and of other similar classes of mechanical systems, and a design method utilizing the models. The model aims to be computationally faster than nonlinear finite element analyses, yet more accurate than the conventional flexible multi-body simulations. The torsion beam is represented as a linkage of lumped mass joined by nonlinear springs, bending and torsion, whose stiffness are identified via off-line computational experiments using nonlinear finite element simulations. A number of such computer experiments are conducted off-line for representative dimensions of torsion beams, and the results are stored in surrogate response models (radial basis function networks), whose inputs are the dimensions of torsion bars and outputs are the corresponding values of lumped masses and nonlinear stiffness of the bending and torsion springs. During design iterations, these surrogate response models are utilized to automatically construct a lumped-compliance linkage model of a torsion beam and integrate it into a multi-body suspension system model that can be simulated using commercial software.

Comparison with a nonlinear finite element analysis demonstrates much improved accuracy of the proposed model over commercial flexible multi-body simulation software, with comparable computational speed. Finally, an example is presented on the multi-objective optimization of the cross section of the torsion beam using the developed surrogate response models.

2. RELATED WORK

2.1. Computational model of torsion beam suspension systems

During the operation of torsion beam suspension systems, large deformation primarily occurs at the torsion beam, whereas the other suspension members mostly behave as a rigid body mechanism. It is therefore naturally modeled as a flexible multi-body system, where the torsion beam modeled as a flexible body is integrated in a multi-body model of other members.

Sugiura *et al.* [4,5] presented a software for automatically generate a reduced stiffness matrix of a torsion bar via Guyan reduction of the finite element model constructed from a cross section drawn on a Excel spreadsheet, and a multi-body model of a suspension system that can be simulated by MSC.ADAMS or a in-house software. Fichera *et al* [6] presented the multi-body model of torsion beam suspension system where the torsion bar is represented as a flexible body integrated in the multi-body model via Ritz method (modal approach), which is also adopted in ADAMS/Flex. Travaglio and Matteo [7] customized ADAMS/Car environment such that the generation

of an ADAMS/Flex model can be easily done without independent FE analyses.

These work, however, assume linear elastic behavior of the torsion beams, which may lead to inaccurate predictions with large displacements. The proposed method aims to remedy this problem by modeling the torsion beam by rigid links connected by nonlinear lumped compliances, whose behaviors are extracted from the surrogate response models trained with the samples of off-line FE analyses.

2.2 Lumped-compliance models for flexible multi-body systems

In order to facilitate the effective exploration of design alternatives, lumped-compliance models have been developed for various applications, such as compliant mechanisms and automotive subsystems.

Since structural members in compliant mechanisms often experience large elastic deformations [8], geometric nonlinearly becomes significant. However, such large deformations are highly localized to the “hinged” ends of slender members, allowing most portions of the members to be seen as rigid links. Pseudo rigid body models [8-12] exploits this fact and models a compliant mechanism as rigid links connected by nonlinear torsion and translational springs. Similar idea has been successfully applied to automotive crashworthiness simulations [13,14], based on the observation that most crash energy is absorbed by beam-like structural frames in a body structure.

These works share many similarities with, and are in fact served as a motivation for, the lumped-compliance model presented in this paper. However, the identification of equivalent nonlinear springs in these works is either done by analytical reduction or numerical observation of the corresponding detailed finite element models, which requires the construction of the detailed model to be examined at each design iteration. To relax this requirement, the present work utilized a surrogate response model that maps physical dimensions of a detailed geometry to equivalent nonlinear springs of a limped compliance model, which are trained off-line by using a small number of design samples.

3. DESIGN OF TORSION BEAM SUSPENSION USING LUMPED-COMPLIANCE LINKAGE MODELS

3.1 Overview

Figure 2 shows an overview of the proposed design method. It utilizes the surrogate models representing the mapping from the cross sectional dimensions of the torsion beam to the lumped masses and inertia and the parameters of the equivalent nonlinear springs. The surrogate models are constructed *off-line* by using the nonlinear FE analyses of torsion beams with representative dimensions. During the optimization loop, the surrogate model receives the candidate cross-sectional dimensions generated by a multi-criteria optimizer. By using the outputs of the surrogate model, the

lumped compliance linkage model corresponding to the cross section is constructed, which is in turn embedded in the multi-body model of suspension system simulated by ADAMS. The simulated elasto-kinematic responses of the suspension system are then fed back to the multi-criteria optimizer. The process iterates until the optimizer terminates with the Pareto optimal cross sectional dimensions with respect to the mass of the torsion beam and the deviation from the target responses.

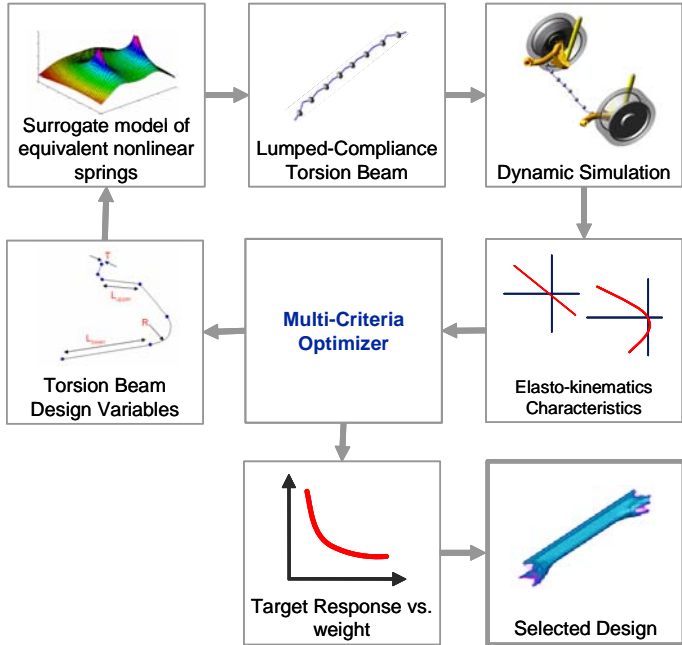


Figure 2. Overview of the proposed design method.

3.2 lumped-compliance linkage model

Lumped compliance linkage model represents a continuum structure as lumped masses and inertia attached to massless linkages and equivalent nonlinear springs attached to the joints connecting the linkages. The load-displacement characteristics of the nonlinear springs are identified via nonlinear FE analyses of the continuum structure model. Since the major deformation modes of the torsion beam during the vehicle operation are longitudinal torsion and bending, only the equivalent nonlinear springs corresponding to these deformations are included.

Figure 3 shows an overview of the construction of a lumped compliance linkage model of a torsion beam from the FE model with detailed geometry. The FE model is decomposed to n sections, each of which will become a link in the lumped compliance linkage model. The number of sections n should be chosen just large enough to accurately model the nonlinear behavior of the torsion beam. In the following case study, $n = 24$ is used. A link is represented as two rigid beams connecting the mass center of the corresponding FE section and the geometric centers of the cross sections at its ends, which we refer to as *hinge* locations. At the mass center, a link has mass and inertial tensor of the

corresponding FE section. Two adjacent links are connected by a ball joint at the hinge location, to which three (nonlinear) torsion springs in x , y , and z directions are attached as illustrated in Figure 4, whose load-displacement characteristics are identified via nonlinear FE analyses of the detailed FE model.

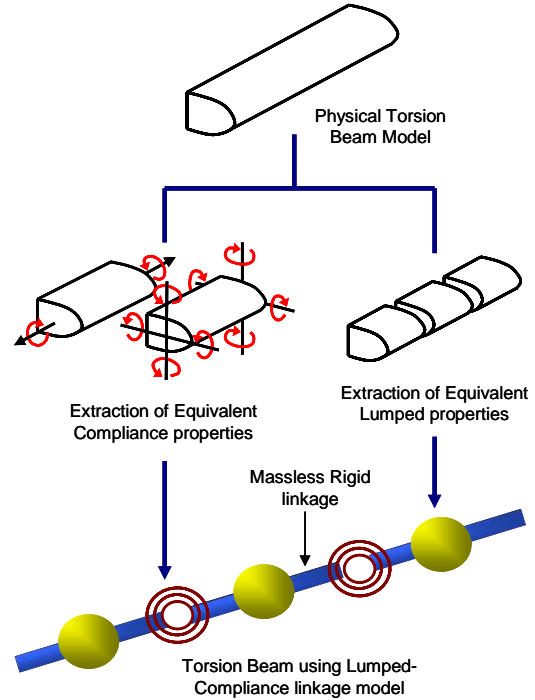


Figure 3. Overview of the construction of lumped compliance linkage model of torsion beam.

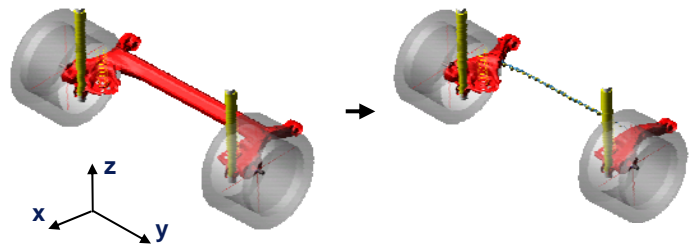


Figure 4. Rear suspension system with lumped-compliance linkage torsion beam.

The equivalent torsion springs in y direction at $n-1$ hinge locations are obtained by the nonlinear FE analysis of the torsion beam subject to longitudinal twist, as shown in Figure 5 (a). The ends of the torsion beam are rigidly connected to their shear centers that are constrained to be allowed only the rotation in y direction. The moments of the same magnitude with the opposite signs are applied at the shear centers, and distortion angles θ_{yi} ($i = 1, 2, \dots, n-1$) at each hinge location as defined in Figure 5 (b) are recorded. The range of the applied moment is determined such that the resulting θ_{yi} is within $\pm 20^\circ$, considering the operating conditions of actual vehicles. Figure

6 shows an example moment-angle plot at a hinge location, as compared to the result of linear FE simulation. As expected, the results of the nonlinear analysis shows strain-hardening effect, which is not captured by the linear analysis. At each hinge location, the equivalent torsion spring in y direction is represented in ADAMS as a spline curve approximating the nonlinear moment-angle relationships such as the one shown in Figure 6.

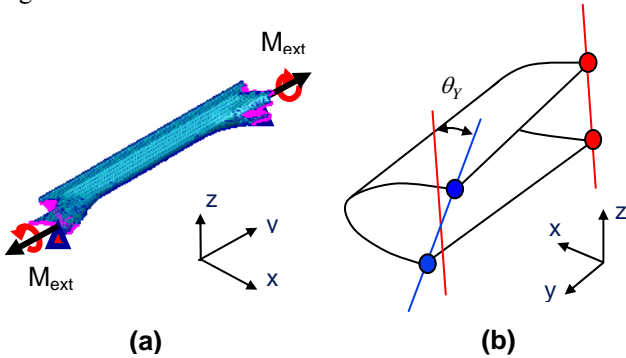


Figure 5. (a) torsion beam subject to twist and (b) definition of distortion angle θ_{yi} .

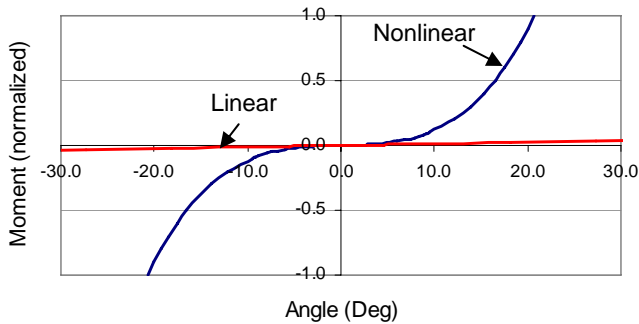


Figure 6. Moment-angle relationship for longitudinal twist of torsion beam

In addition to distortion angle θ_{yi} , the reacting torque in x and z directions at the shear centers where moment are applied are also recorded. These reacting torques are utilized to simulate the warping of the torsion beam due to the coupling of longitudinal twist and bending. However, the subsequent analysis showed the effect of warping on suspension responses is extremely small, and hence these reaction torques are not included in the lumped compliance linkage model.

The equivalent torsion springs in x and z directions are obtained by the nonlinear FE analysis of a half of the torsion beam subject to longitudinal bending, whose one end (the middle of the entire torsion beam) is fully constrained and the other end is rigidly connected to its shear center just like the case in Figure 5 (a). For each of x and z directions, force or moment is applied to the shear center, and the respective distortion angles θ_{xi} and θ_{zi} ($i = 1, 2, \dots, n-1$) at each hinge locations as defined in Figure 7 are recorded. It should be noted the moment-angle curve obtained by applying force and the curve obtained by applying moment do not coincide for small

n , although both curves are almost linear owing to the straightness of the torsion beam. Figure 8 shows example stiffness (slope of moment-angle curve)-moment plots at a hinge location in the case of $n = 24$, which indeed exhibit such a discrepancy. Since the stiffness, obtained from either force or moment, is almost constant at a hinge location regardless of the magnitude of the applied bending moment, their averages are taken as the equivalent bending stiffness k_{xi} and k_{zi} in x and z directions at hinge i , as shown in the thick line in Figure 8. These springs are simply represented as linear torsion springs in ADAMS.

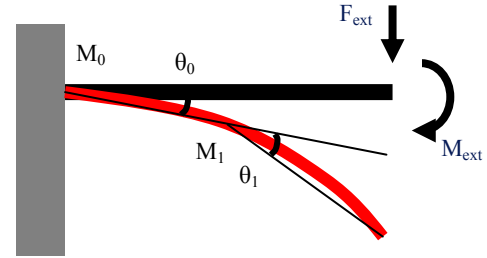


Figure 7. Definition of distortion angles for bending. Simplified 2-section beam is used for clarify.

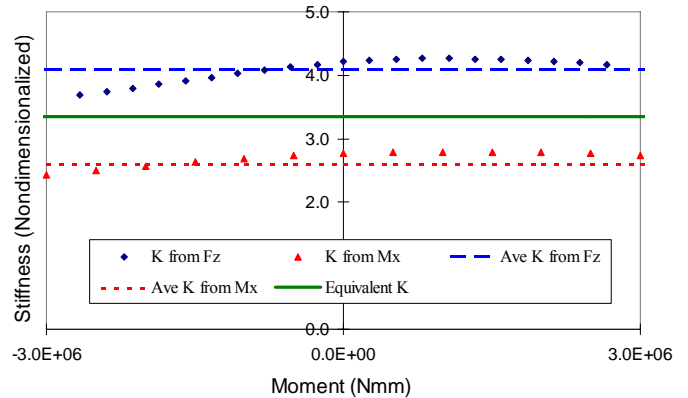


Figure 8. Stiffness-moment relationship for longitudinal bending of torsion beam

3.3 Validation of lumped-compliance linkage model

The responses of the lumped compliance linkage model of a torsion beam simulated by ADAMS are compared with the ones of a FE model of the same torsion beam simulated by nonlinear FE analysis with NASTRAN. Figure 9 shows the distortion angle θ_y at an end of the torsion beam as a function of applied moment, obtained by the lumped compliance linkage model and the nonlinear FE model. As clearly seen in the figure, both results closely match each other.

Next, the responses of the multi-body suspension system model integrating the lumped compliance linkage model are compared with the ones 1) of a detailed FE model of the same suspension system with simplified bushings, shock absorbers, and tires, and 2) of a flexible multi-body (ADAMS/Flex) model that represents the torsion beam and trailing arms as a single flexible component. Although such system level comparison

should ideally done with the test data of a physical suspension system, the nonlinear FE analysis was used as a baseline due to the lack of available data. The models are simulated with the wheel stroke input for Kinematic Alternative Stroke Test [2] shown in Figure 10. During the simulations, camber angle, toe angle, and the trajectory of spindle in x direction are recorded as response measures, whose definitions are given in Figure 11.

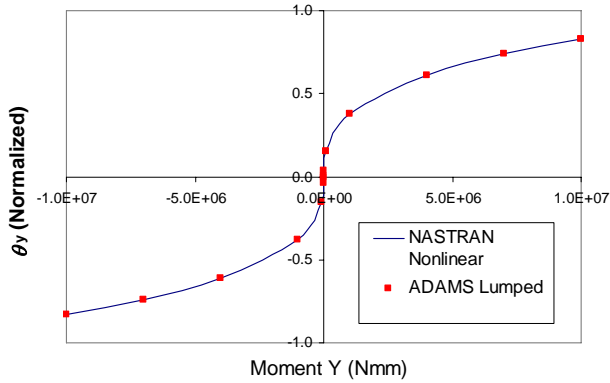


Figure 9. Comparison of distortion angle θ_y .

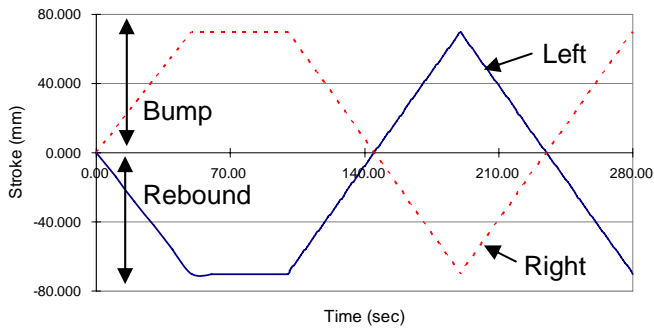


Figure 10. Wheel stroke input for Kinematic Alternative Stroke Test.

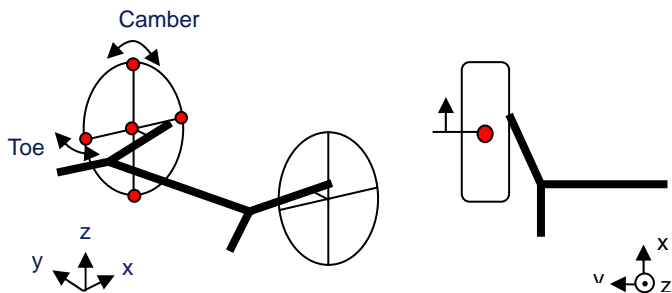


Figure 11. Definitions of response measures: (a) camber and toe angles and (b) trajectory of spindle in x direction.

Figure 12 shows the simulation results. The results by the lumped compliance linkage model match well with the results by the nonlinear FE model except for the toe angle. For the toe angle, the nonlinear FE model shows rather unrealistic results and hence should not be seen as a reference for accuracy in simulating toe angles. This unrealistic toe angle is perhaps due

to the shell elements parallel to the x - y plane (the plane on which the toe angle is measured), which exhibit too stiff behaviors in the plane. On the other hand, the toe angles by the flexible multibody model and lumped compliance linkage model exhibit the same trend. The lumped compliance linkage model captures well the nonlinear behavior for the trajectory of spindle in x direction, which the flexible multibody model failed to simulate. The comparison of computational speed is presented in Figure 13, where the lumped compliance model shows almost five fold improvement over the flexible multibody model. This is because the lumped compliance linkage model does not require simulating flexible components, which can add significant computational overhead.

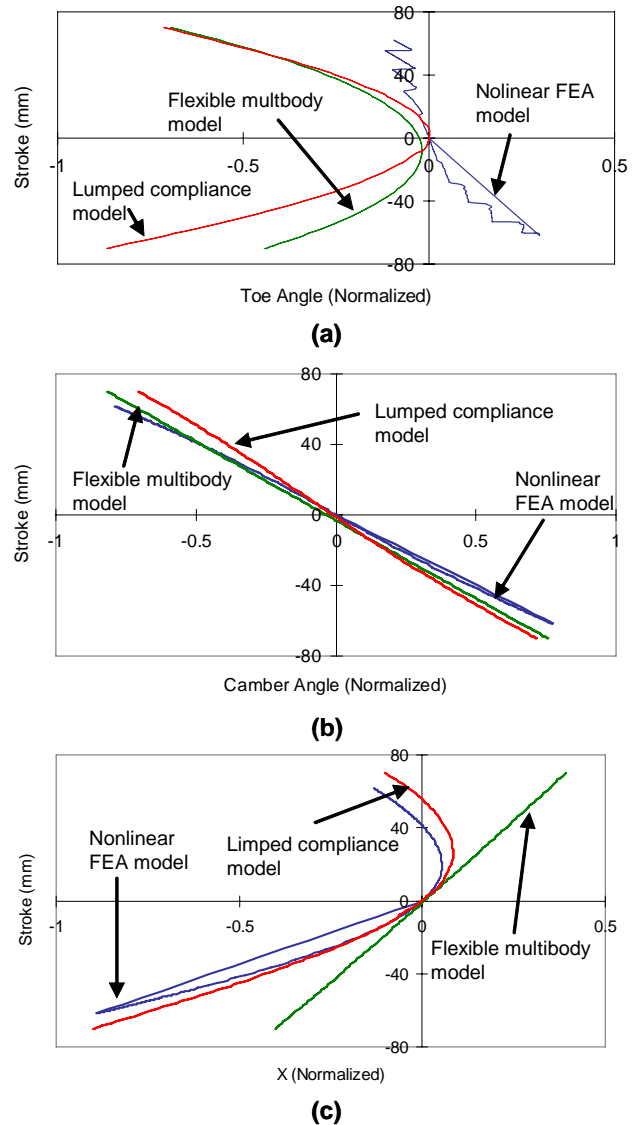


Figure 12. Comparison of responses: (a) toe angle, (b) camber angle, and (c) trajectory of spindle in x direction.

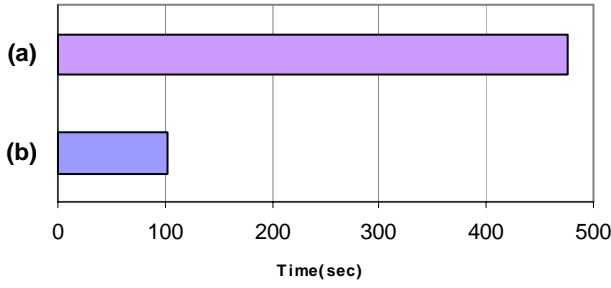


Figure 13. Comparison of computational speed: (a) flexible multibody model, and (b) lumped-compliance linkage model.

3.4 Surrogate Model

Since the identification of equivalent nonlinear springs requires the nonlinear FE analyses of a torsion bar model with detailed geometry, it is undesirable to go through the construction process in Figure 2 each time design changes are made. As such, nonlinear springs for torsion beams with a number of representative dimensions are identified *a priori*, and surrogate response models are built based on the information.

These surrogate models (radial basis function network [15]) take as inputs the cross sectional dimensions of the torsion beam shown in Figure 14 and output the following quantities:

- mass center location (x_{mi}, y_{mi}, z_{mi}) of link $i = 1, 2, \dots, n$.
- hinge location (x_{hi}, y_{hi}, z_{hi}) of hinge $i = 1, 2, \dots, n-1$
- lumped masses m_i of link $i = 1, 2, \dots, n$.
- lumped inertia $I_{ixx}, I_{iyy}, I_{izz}, I_{ixy}, I_{iyz},$ and I_{ixz} of link $i = 1, 2, \dots, n$.
- stiffness k_{xi} , and k_{zi} of the equivalent linear torsion spring in x and z directions, respectively, at hinge location $i = 1, 2, \dots, n-1$.
- parameters $k_i, a_i, b_i, c_{i1},$ and c_{i2} as defined in Equation 1 and Figure 15, which describe the moment-angle curve of the equivalent nonlinear torsion spring in y direction at hinge location $i = 1, 2, \dots, n-1$.

$$f(x) = \begin{cases} kx & 0 \leq x < c_1 \\ \frac{c_2 - x}{c_2 - c_1} kx + \frac{x - c_1}{c_2 - c_1} ax^b & c_1 \leq x < c_2 \\ ax^b & c_2 \leq x \end{cases} \quad (1)$$

The locations of mass center and hinge, and lumped mass and inertia are computed from the corresponding FE section, and the properties of equivalent torsion springs in x, y, z directions are obtained by the nonlinear FE simulations of the entire torsion beam as described in the previous section. The

surrogate models are trained by 25 sample input-output pairs in the feasible ranges of input variables, generated by using Design of Experiment with Box-BehnKen design [16].

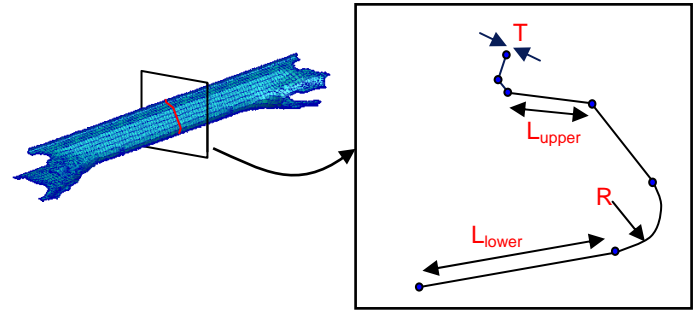


Figure 14. Dimensions of torsion beam cross section selected as design variables.

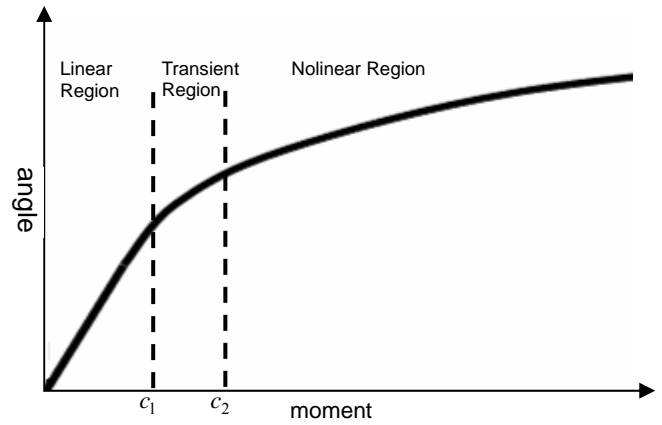


Figure 15. Parameterization of moment-angle curve of torsion spring in y direction.

The accuracy of the surrogate model was validated by two random designs not among the training samples. For each of these designs, two lumped compliance linkage models of the entire suspension system are constructed, one using the parameters predicted by the surrogate model, and another using the parameters extracted from nonlinear FE simulation. Table 1 shows the root square mean error (RSME) of the responses from these models, which show the prediction by the surrogate model is sufficiently accurate.

Table 1 Root Square Mean Error of responses of surrogate model and actual model

Toe Angle	Camber Angle	Trajectory of spindle in x direction
0.0084	0.0174	0.0089

3.5 Simulation and Optimization

For given values of the cross sectional dimensions in Figure 11, the surrogate model outputs the parameters necessary for constructing the lumped compliance linkage model, based on which an ADAMS model of the suspension

system embedding the lumped compliance linkage model is generated. Software is developed for visualizing the input cross sections, generating an ADAMS model by calling the surrogate models, simulating the model with ADAMS, and collecting and displaying the simulation results. Figure 16 shows the graphical user interface (GUI) of the developed software, Flexsus.exe, designed for the interactive exploration of design alternatives.

The software can also be used in a batch mode with file I/O, so that it can be integrated with an external optimizer. In the following case study, iSIGHT 8.0 from Engineous Software is used. A multi-objective genetic algorithm NSGA-II [17] is chosen as an optimization algorithm in order to obtain Pareto optimal designs with respect to the mass of the torsion beam and the deviation from the target responses, which tends to prefer heavy torsion beam.

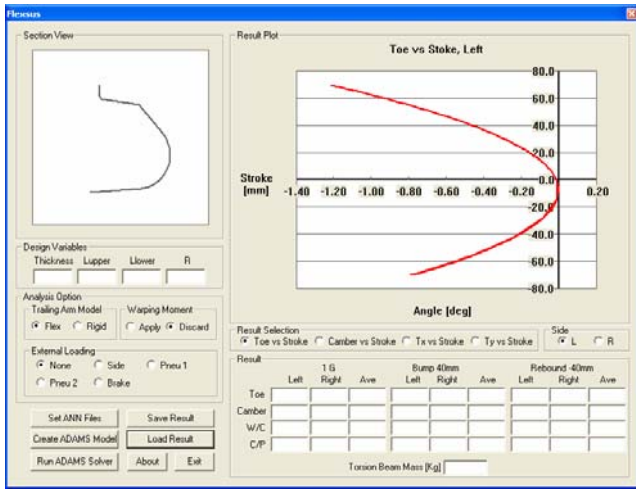


Figure 16. Graphical user interface of Flexsus.exe.

4. CASE STUDY

4.1 Optimization problem

Using the developed software, a case study is conducted on the optimization of the cross section geometry of the torsion beam. Design variables \mathbf{x} are the cross sectional dimensions in Figure 14:

$$\mathbf{x} = (L_{upper}, L_{lower}, T, R) \quad (2)$$

There are two objectives to be minimized. The first objective is the mass of the torsion beam:

$$f_1(\mathbf{x}) = \sum_{i=1}^n m_i \quad (3)$$

where n is the number of links and m_i is the lumped mass of the i -th link of the lumped compliance model of the torsion beam.

The second objective is the deviation of the responses of the suspension system model from the target responses, computed as the weighted sum of the distances to the targets:

$$f_2(\mathbf{x}) = \sum_{i=1}^{n_r} w_i |r_i(\mathbf{x}) - \rho_i| \quad (4)$$

where n_r is the number of responses, $r_i(\mathbf{x})$ and ρ_i are the i -th response and target, respectively, and w_i is the weight of the i -th target, which are chosen so terms in the sum are approximately the same in magnitudes. In the case study, the following four responses are measured by simulating Kinematical Alternative Stroke Test in Figure 10:

1. **Bump Toe:** Average toe angle over the bump with +40 mm stroke input.
2. **Bump Camber:** Average camber angle over the bump with +40 mm stroke input.
3. **Rebound Toe:** Average toe angle over the rebound with -40 mm stroke input.
4. **Rebound Camber:** Average camber angle over the rebound with -40 mm stroke input.

and the target values of these responses are given in Table 1.

Table 2 Target responses for optimization case study.

Bump Toe [deg]	-0.45
Bump Camber [deg]	-2.40
Rebound Toe [deg]	-0.16
Rebound Camber [deg]	2.40

In summary, the following two-objective optimization problem is solved:

$$\begin{aligned} &\text{minimize} && \{f_1(\mathbf{x}), f_2(\mathbf{x})\} \\ &\text{subject to} && \mathbf{x}_l \leq \mathbf{x} \leq \mathbf{x}_u \end{aligned}$$

Due to a proprietary reason, the values of the design variables are shown as normalized to [-1, 1] in the following discussions. The above problem was solved by using NSGA-II available in iSIGHT 8.0, with the population size being 50 and the number of generations being 50. It took slightly less than 26 hours with a 3.2 GHz Windows PC.

4.2 Results

Figure 17 shows the population at the last generation of NSGA-II shown in the objective function space, where Pareto optimal solutions are indicated as dark circles. The results indicate a clear trade-off between the mass of the torsion beam and the deviation from the target value. Since all responses are elasto-kinematic and their targets are set as small values, stiff (and hence heavy) designs tend to achieve smaller deviation from the targets.

Three representative designs, A, B, and C are selected among the Pareto optimal designs in Figure 17 to examine the trade-off between the objective functions and its relation to the cross sectional dimensions. The values of the objective functions and the design variables of these designs are shown in Table 1.

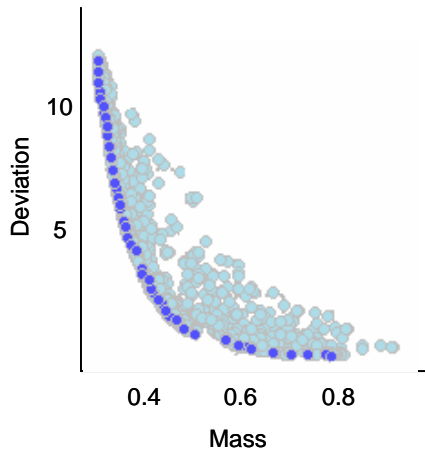


Figure 17. Population at last generation of NSGA-II. Pareto optimal solutions are darkened.

Table 3. Summary of designs A, B, and C.

	f_1 (mass)	f_2 (deviation)
Design A	0.342	11.862
Design B	0.862	0.144
Design C	0.534	1.214

	T	L_{upper}	L_{lower}	R
Design A	-1.000	-0.808	-0.641	0.349
Design B	0.175	0.296	0.948	-0.535
Design C	-0.997	0.336	0.992	-0.567

Figure 18 shows design A, which has the minimum mass and the maximum deviation from the targets. This design has very small T (almost at the lower bound) and small L_{upper} and L_{lower} values, realizing the 40% mass reduction from the baseline design examined in Section 3. However, the resulting torsion beam is too compliant, showing in very large deviation from the targets

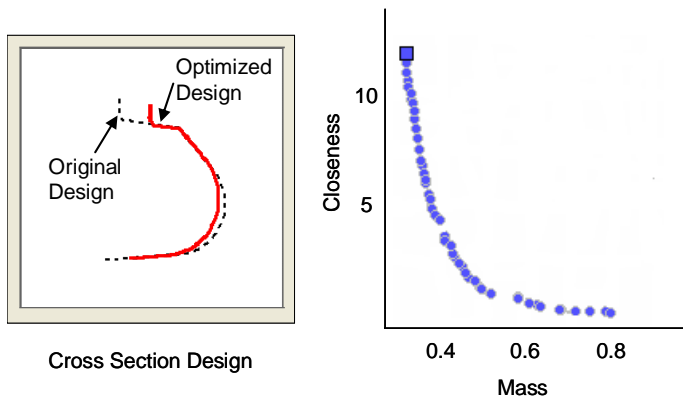


Figure 18. Design A with minimum mass.

Figure 19 shows design B, which has the minimum deviation from the targets and the maximum mass. This design has very small R (almost at the lower bound) and large values

for other design variables. This causes a large polar 2nd moment of inertia and in turn large torsion stiffness, which ultimately realizes the 93% reduction of the deviations from the targets compared to the original design examined in Section 3. However, the resulting torsion beam is too heavy, which may negatively impact the dynamic performance of the suspension system.

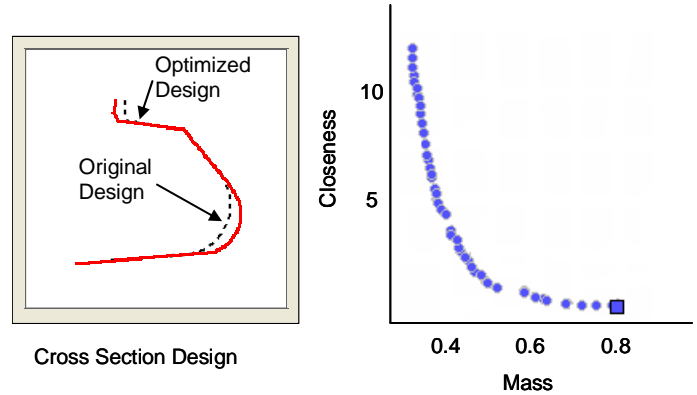


Figure 19. Design B with minimum deviation from target responses.

Figure 20 shows design C, which exhibits a well balanced compromise between two objectives. The design is very similar to design B in Figure 18, except that the thickness is much smaller than design B. Compared to the original design examined in Section 3, the deviation from the targets is improved by 46% while the mass is also decreased by 10%. Figure 21 shows responses of lumped compliance linkage model and nonlinear FEA model corresponding design C. Similar to the comparison done in Section 3.3, toe angle response of the nonlinear FEA model is unrealistic, and vastly different from one of the lumped compliance linkage model. On the other hand, they match well for camber angle. Based on the similarity in trends to the comparison in section 3.3, it would be fair to conclude that the interpolation by the surrogate model at design C is sufficiently accurate.

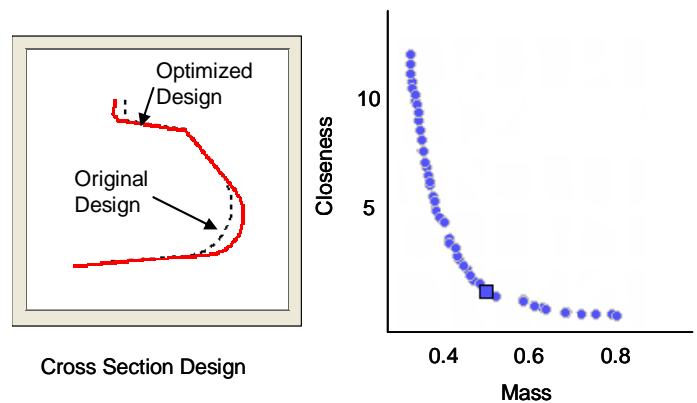


Figure 20. Design C with well balanced compromise between two objectives.

5. CONCLUSION

A lumped compliance linkage model of the torsion beam in a suspension system allows the efficient and accurate simulation of the elasto-kinematic behavior via simple multi-body simulation without using flexible bodies. By constructing the surrogate models that maps the cross sectional dimensions of the torsion beam to the properties of the lumped compliance models, it enables both interactive design examination and batch-mode optimization of the torsion beam suspension systems.

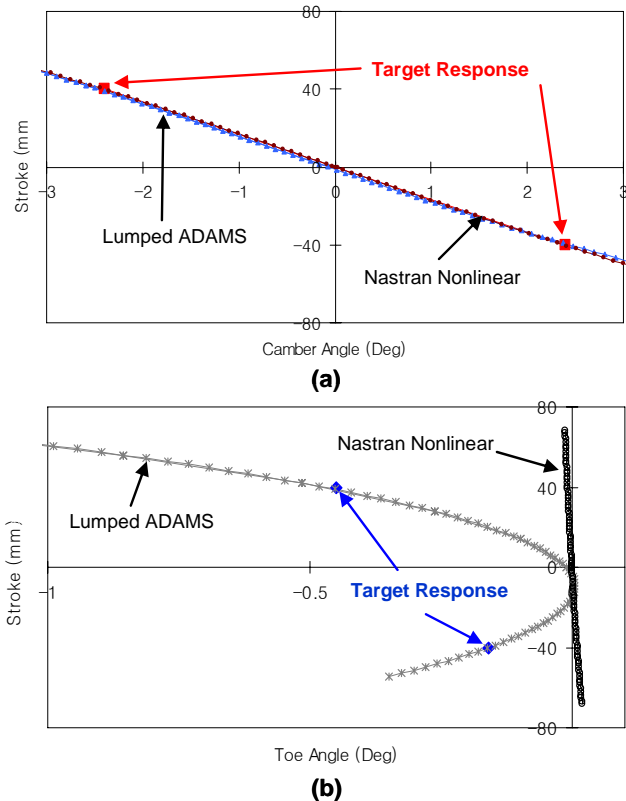


Figure 21. Comparisons of responses of Design C: (a) Camber angle and (b) Toe angle

ACKNOWLEDGEMENTS

The funding for this research was provided by the Honda R&D Co. Ltd. The license for iSIGHT is provided by Engineous Software, Inc. through the educational program. These resources are gratefully acknowledged.

REFERENCES

- [1] MSC.ADAMS, <http://www.mscsoftware.com>
- [2] Bastow, D., Howard, G., Whitehead, J. P., 2004, *Car Suspension and Handling*, 4th ed. SAE International, Warrendale
- [3] Saitou, K., 2004, "First Order Analysis as designer's model: introductory remarks and overview," Special session on First Order Analysis (FOA), Proceedings of

the SAE 2004 World Congress, Detroit, Michigan, March 8-11.

- [4] Sugiura, H., Nishigaki, H., Nishiwaki, S., Kojima, Y., and Arima, M., 2000, "First Order Analysis for automotive chassis design – application to torsion beam suspension," *SAE Technical Paper 2000-08-0097*, Society of Automotive Engineers, Pennsylvania.
- [5] Sugiura, H., Kojima, Y., Nishigaki, H., Arima, M., 2000, "Trailing twist axle suspension design using ADAMS," Proceedings of the *FISTA World Automotive Congress F2000G306*.
- [6] Fichera, G., Lacagnina, M., and Petrone, F., 2004, "Modeling of torsion beam rear suspension by using multibody method," *Multibody System Dynamics*, 12(4), pp. 303-316.
- [7] Travaglio, G. C., Matteo, L., 1999, "Optimising the Handling Behaviour of a Vehicle with McPherson Front Suspension and Twist Beam Rear Suspension Using ADMAS/CAR," *ADAMS User Conference*
- [8] Saxena, A. and Kramer, S. N., 1998, "A simple and accurate method for determining large deflections in compliant mechanisms subjected to end forces and moments," *Journal of Mechanical Design*, 120(3), pp. 392-400.
- [9] Chang, R. J. and Wang, Y. L., 1999, "Integration method for input-output modeling and error analysis of four-bar polymer compliant micromachines," *Journal of Mechanical Design*, 121(2), pp 220-228.
- [10] Saggere, L. and Kota, S., 2001, "Synthesis of planar, compliant four-bar mechanisms for compliant-segment motion generation," *Journal of Mechanical Design*, 123(4), pp. 535-541.
- [11] Edwards, B. T., Jensen, B. D., and Howell, L. L. A., 2001, "Pseudo-rigid-body model for initially-curved pinned-pinned segments used in compliant mechanisms," Technical Brief, *Journal of Mechanical Design*, 123(3), pp. 464-468.
- [12] Kimball, C. and Tsai, L.-W., 2002, "Modeling of flexural beams subjected to arbitrary end loads," *Journal of Mechanical Design*, 124(2), pp. 223-235.
- [13] Nishigaki, H. and Kikuchi, N., 2004, "First Order Analysis of automotive body structure design part 3: crashworthiness analysis using beam elements," *SAE Technical Paper 2004-01-1660*, Society of Automotive Engineers, Pennsylvania.
- [14] Hamza, K. and Saitou, K., 2005 "Design for Structural Crashworthiness using Equivalent Mechanism Approximations," *Transactions of the ASME, Journal of Mechanical Design*, 127(3), pp.485-492.
- [15] MathWorks, 2001, *MatLab 6 Documentation*, MathWorks Inc., Natick, MA.
- [16] Box, G. E. P., Hunter, W. G., and Hunter, J. S., 1978, *Statistics for Experimenters: An Introduction to Design, Data Analysis, and Model Building*, John Wiley & Sons, New York.

- [17] Deb., K., Agrawal, S., Pratab, A., and Meyarivan, T., 2000., "A Fast Elitist Non-Dominated Sorting Genetic Algorithm for Multi-Objective Optimization: NSGA-II", KanGAL report 200001, Indian Institute of Technology, Kanpur, India.